

# AM-CCA: A Memory-Driven System for Fine-Grain and Dynamic Computations

Bibrak Qamar Chandio, Prateek Srivastava, Maciej Brodowicz, and Thomas Sterling

*Department of Intelligent Systems Engineering*

Indiana University Bloomington, USA

Email: {bchandio, pratsriv, mbrodowi, tron}@iu.edu

**Abstract**—Techniques of computer systems that have been successfully deployed for dense regular workloads fall short of achieving their goals of scalability and efficiency when applied to irregular and dynamic applications. This is primarily due to the discontent between the multiple layers of the system design from hardware architecture, execution model, programming model, to data-structure and application code. The paper approaches this issue by addressing all layers of the system design. It presents and argues key design principles needed for scalable and efficient dynamic graph processing, and from which it builds: 1) a fine-grain memory driven architecture that supports asynchronous active messages, 2) a programming and execution model that allows spawning tasks from within the data-parallelism, 3) and a data-structure that parallelizes vertex object across many compute cells and yet provides a single programming abstraction to the data object.

Simulated experimental results show performance gain of geometric  $2.38\times$  against an state-of-the-art similar system for graph traversals and yet being able to natively support dynamic graph processing. It uses programming abstractions of actions, introduces new dynamic graph storage scheme, and message delivery mechanisms with continuations that contain post-completion actions. Continuations seamlessly adjusts, prior or running, execution to mutations in the input graph and enable dynamic graph processing.

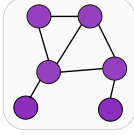
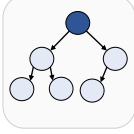
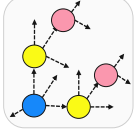
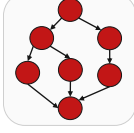
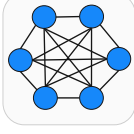
## I. INTRODUCTION

Commonly, when new computer architectures are developed, they are reasoned in terms of a dichotomy called the hardware-software co-design. This reasoning presumes other key aspects of the entire system to be the default, mostly the execution model. Consequently, little effort is devoted to comprehensively addressing and exploring the ideas and mechanisms that form the entirety of the new computing system.

This paper tries to approach the problem of designing a highly parallel and scalable computing system for dynamic and fine-grain computations such as dynamic graph processing. One way to move beyond hardware-software co-design dichotomy is to look at various forms that graphs take in a computing system. There can be five different forms as manifestations of: representation, programming, processing, and computer system structure. Table I provides further details.

Instead of treating these manifestations as separate entities and performing incremental advancements, we ask the question whether we can take an approach into unifying these manifestations in a hope to potentially come up with candidate designs of a computing system that is inherently build for

TABLE I: Graph Manifestations

Graph Type and Properties	
	<b>Data graph</b> <ul style="list-style-type: none"> <li>• It contains the input data.</li> <li>• Parallelism intrinsic in topology.</li> <li>• Static or dynamic.</li> <li>• Regular or irregular (variable degrees).</li> </ul>
	<b>Data-structure of the Data graph</b> (A Single Recursively Parallel Vertex shown) <ul style="list-style-type: none"> <li>• Adjacency List or Adjacency Matrix.</li> <li>• Vertex objects using pointers. A single vertex can be partitioned hierarchically in a tree and operated upon using recursive parallelism.</li> </ul>
	<b>Program graph</b> (BFS shown) <ul style="list-style-type: none"> <li>• Dataflow graph.</li> <li>• Programmer describing the algorithm.</li> <li>• Compiler further changes/adapts it.</li> </ul>
	<b>Execution graph</b> (DAG shown) <ul style="list-style-type: none"> <li>• Variable with respect to each instance.</li> <li>• Dynamic due to runtime control.</li> <li>• Time dependent.</li> </ul>
	<b>Architecture graph</b> (Dragonfly topology shown) <ul style="list-style-type: none"> <li>• Network-on-Chip.</li> <li>• System area network topology.</li> <li>• Routing Algorithms.</li> </ul>

scalable dynamic fine-grain computations. Within this context, the paper describes key design principles and an exploratory approach to develop and study architectures, asynchronous programming model and runtime systems, along with data structures for irregular and dynamic computations for scalable and efficient graph processing. We call our design the Active-Memory Continuum Computer Architecture (AM-CCA).

### A. System Design Principles

We argue that the following system design principles have the potential to enable scalable fine-grain parallelism for irregular and dynamic computations.

1) *Memory model*: Physical memory must be logically unified with the data contained in it. It is a shift from a segregated view of data that is contained logically within processes, which

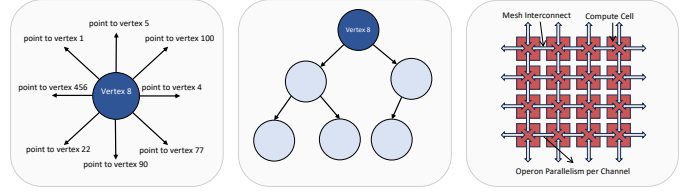
in turn reside within a physical memory space that is fractured into caches, NUMA domains and nodes. Instead, compute logic must be organized around memory thereby making a memory centric model. This physical memory layout must be homogeneous and unified at the logical level by objects that not just represent data state but also the action state and the logical hierarchy as represented by the references between data objects (logical locality). Section III and Section IV use this principle to design hardware mechanism and vertex data structure, respectively.

2) *Communication and Programming model*: The communication must be unified by creating a global and shared communication network that is built for large number of small messages thereby optimizing for latency. This is a departure from staging data at various levels of hierarchies to optimize for bandwidth and enforcing different, and mostly static and synchronous, control flow mechanism. To export high degrees of parallelism and hide latency the communication must be made transparent and captured though the asynchronous and dynamic parallel programming semantics that can enable spawning computations from within data object. Section V uses this principle to design the programming model that spawns dynamic computations by moving “work to data” in the form of active messages for fine-grain compute and communication parallelism.

3) *Execution Model*: The execution model must allow global parallelism. Most contemporary computing architectures are based on von Neumann sequential machines that are connected together, thereby creating what is called the Communicating Sequential Processes (CSP) execution model. Such machines may have high degrees of local parallelism, but in practice, they employ globally sequential methods. Section II-A further discusses some important prior work in this regard. Section III inherits some of these ideas in designing the hardware structure of AM-CCA, and Section V for the programming model.

4) *Diversity of Parallelism*: Graphs do not have well-structured spatial locality patterns and therefore techniques such as data-parallelism do not inherently scale well. Data-parallelism techniques are generally very static and regular, requiring data that is not only spatially contiguous but also remains unchanged once the computation begins. This is also coupled with the fact that graph operations are not highly compute intensive. Consequently, control (or task) parallelism techniques, such as those under fork-join and Bulk Synchronous Parallel (BSP), incur significant synchronization overheads and execution irregularities. New approaches to forms of parallelism should be explored that combine aspects of data parallelism and control parallelism, thereby broadening Flynn’s Taxonomy [14] and Duncan’s taxonomy [9]. These may include:

**Meta-Data Parallelism**: Control-parallelism could work on meta-data of the irregular structure and expose inherent parallelism. It can be achieved by placing data (the graph structure) near computing capabilities that have the ability to dynamically spawn more computations. Such a setup will



(a) An input graph (b) A single vertex (c) Dense compute  
vertex contains meta- can be partitioned cell tessellation cre-  
data such as edges hierarchically and ates *operons* enabling  
that can be exposed at placed across multiple large amount of mem-  
runtime for meta-data compute cells to allow ory operations in par-  
allelism. recursive parallelism. allel.

Fig. 1: Types of Parallelism employed by AM-CCA.

allow computations to asynchronously originate from within the graph vertex and diffuse throughout the larger graph. Figure 1a shows a vertex containing edges that are the meta-data interpreted as parallelism. It is a departure from conventional data-parallelism where a central (“mother”) computation stages the operations and then uses some form of distributed (yet synchronized) control-parallelism to take the processing through its various stages. Section V uses this idea to write programs that dynamically spawn new actions (active messages) along the edges of the data graph.

**Recursive Parallelism**: Entities that may include graphs, lambda expressions, and algorithmic processes, can be constructed with inherent recursive structure and then allocated across multiple compute capable memory cells (called Compute Cells of AM-CCA) that have the ability to perform computation locally. The recursive structure coupled with its distribution on large number of active memory cells will not only provide another mode of parallelism but will also, when used in conjunction with other modes of parallelism, especially meta-data parallelism, can further extract parallelism out of any single data object.

For example, a graph processing task (or algorithm) is executed using meta-data parallelism and simultaneously at the vertex level each vertex spawns recursive parallelism, because the vertex itself is recursively partitioned and constructed, as shown in Figure 1b. Section IV uses these ideas to form the Recursive Parallel Vertex Object (RPVO), which dynamically grows or shrinks a single vertex object across multiple active memory cells and parallelizes operations on a single vertex object. Specially useful for skewed degree distribution vertices.

**Operon Parallelism**: An operon is a mechanism, similar to an active message, by which actions or instructions are sent to a remote locality that hosts the data. Figure 2 shows the structure of an operon. A fine-grain memory-driven system can have *operons* can be in flight simultaneously. In this way high memory-ops concurrency can be expose and then exploited by the underlying network and the active memory system.

For example, as illustrated in Figure 1c, within square tessellated compute cells, there are four out-degree channels. Depending on the routing scheme, these channels can concurrently transmit four distinct *operons*. As a result, in a Torus-



Fig. 2: Structure of an operon. Contains source and destination compute cell addresses for routing. The action, containing instructions, along with its payload, which can be operands. Operons have an additional continuation specifier which contains post-completion actions that distinguishes it from “active messages”. We use continuations to implement dynamic graph processing.

Mesh topology there are  $4 \times N^2$  channels transmitting *operons*. Section III uses operon as the logical transmission unit for *action* delivery.

## II. PRIOR TECHNIQUES AND THEIR SYNTHESIS

This section discusses some of the past contributions, techniques, and ideas that we believe have the potential to be synthesized to enable future scalable, fine-grain, and dynamic computational models and architectures.

### A. Theoretical Works

Typically, contemporary computing systems are conceived under the sequential process computing model, where instructions are issued one at a time. Although local optimizations such as superscalar, pipelines, out-of-order execution, and branch prediction have been made to extract parallelism and are coupled with the CSP model for scaling, nevertheless, there still remains an inherent lack of global parallelism at scale.

Functional and concurrent models provide unbounded parallelism and can be synthesized, especially utilizing the properties of lambda calculus [5], actors model [18] [2] and cellular automata [36]. For example, currying in lambda calculus has the properties of:

- 1) Allowing the computation to progress while waiting on some arguments to be available.
- 2) Allowing the runtime context of the computation to be stored and potentially migrated to some other part of the larger physical computing machine.

The above two properties are of interest to problems that arise out of the irregular, fine-grain and dynamic nature of graph processing. These can be used to: 1) increase throughput of the system by evaluating computations and not waiting on some dependencies, and 2) migrate computations to improve load balance of the system and also hide latency by migrating computation to where the data resides.

Properties of the actors model include being history-sensitive (unlike dataflow functional systems) and being able to gracefully deal with dynamic topology, thereby making it re-configurable and extensible. From both a structural and functional point of view, cellular automaton provides neighborhood state transforms, which can inspire future class of Processing In Memory (PIM) architectures. These can be used to further evaluate the placement, capacities and capability, and interaction of compute and memory logic. Section III

contains details about these ideas and their incorporation into AM-CCA.

Linial’s LOCAL model [24] studies graph algorithm that can provide an output based on the local vertex data and the data surrounding a smaller neighborhood in the graph topology. It models the computations as if the vertex has some processing ability and can send and receive messages from their neighbors. In this way the LOCAL model theoretically studies graph algorithms as if the graph were executing itself. In the language of computer architecture, this appears to be close to some form of PIM-styled message-driven computing system.

### B. Architecture and Machines

High-Level Language Computer Architectures (HLLCA) [8], such as Intel iAPX [31], and knowledge-based systems like the NETL architecture [11] [10] provide native support for garbage collection and application representation (think of the `list` in Lisp). HLLCAs also incorporate tagged memory [12], which enables a single operation or instruction to handle many types, resulting in compact code representation [15]. Tagged memory maybe more important for message-driven systems that send work to data. AM-CCA can benefit by having smaller code size for operon movement. The prior work and ideas of HLLCAs can be used to unite the application, compiler, OS, and the architecture for runtime introspection and on the fly optimization, which is a unique demand for dynamic and irregular applications like dynamic graph processing.

Furthermore, PIM architectures not only provide an answer to the von Neumann bottleneck, but also together with capabilities such as execution migration, of active messages [33], parcels and thread percolation [32], can explore more fine-grain parallelism and hide latency. These along with the Dataflow architectures’ properties of exposing fine-grain parallelism, through the program control graph [4], and J-Machine’s [28] built-in support for fine-grain asynchronous messaging and a system model for actors, can provide a way towards uniting data parallelism with control parallelism.

Tesseract [3] uses 3D stacked technology the Hybrid Memory Cube (HMC) to further the promise of PIM. Graph data can reside on any cube and can be referenced or mutated by the means of function invocation. These function calls can be blocking or non-blocking. In the latter case, the programmer must ensure global barrier synchronization to guarantee whether a non-blocking call finished. This implies that Tesseract implements the BSP model and can be challenging to implement globally asynchronous regimes.

Dalorex [29] is a cache-less architecture, where new tasks spawn at each memory indirection. These tasks are then sent for execution to the cores where the data resides. Dalorex’s programming model and execution can support fully asynchronous computations without any global barriers. We provide a detailed comparison of AM-CCA with Dalorex in Section VI-D.

### C. Networking Infrastructure and Algorithms

Fine-grain computations impose different kind of challenges on achieving a scalable networking infrastructure. These include the ability to:

- 1) Allow small size messages to be sent with low latency; as sending messages in bulk or blocking communication can reduce the amount of parallelism exposed.
- 2) Allow large number of small messages; the network must be able to sufficiently deal with resources waiting for contention.
- 3) Route a large number of small messages in a smaller number of hops.

Networks such as the Data Vortex, and low diameter topologies such as Kautz, and PolarFly [23] try to address these three challenges. Data Vortex provides a low latency and contention free network [34] that is important for implementing message-driven fine-grain architectures at scale. The Kautz and PolarFly topologies provide the properties of small diameter needed to route messages in a small number of hops. The data graphs themselves have diameters and the idea is to provide the architecture graph the capability to physically traverse the diameter in as little hops as possible (comparing the logical data graph diameter). On the other hand, more pertinent to the scope of this paper, is the network-on-chip (NoC). For example, the most common NoC, the mesh, although high in bandwidth, suffers from high latency due to its larger diameter. This can be mitigated with techniques such as wrapping around the borders to form Torus-Mesh, or adding extra links to the mesh topology such as the Ruche networks [19], thereby lowering the diameter and effectively the latency. AM-CCA uses a Torus-Mesh without relying on Ruche networks and yet scale at larger chip sizes. Section VI-D provides details about strong scaling of AM-CCA.

### III. HARDWARE DESIGNS

The AM-CCA is inspired by the Continuum Computer Architecture (CCA) [6] and is organized as an interconnection of homogeneous global memory Compute Cells (CCs), which are capable of; 1) data storage; 2) data manipulation; and 3) data transmission to adjacent CCs. Figure 3 provides block diagram of a CC that show its interconnect links that interface its operon handler, a limited capacity of data storage and other resources for instruction execution. Since a CC has a limited amount of memory, an arrangement of CCs tessellated, shown in Figure 4, for tight coupling, and interconnected work together to provide logical unification, unbounded data storage capacity and parallelism. Such an interconnect, in its simplest form, is a mesh network, and will be based on shape of the tessellation. The actual number of CCs, their capacity and capabilities, and the mesh arrangement is a design objective to optimize for, and dependent on technology and application behavior. This section explores the design space at the hardware level.

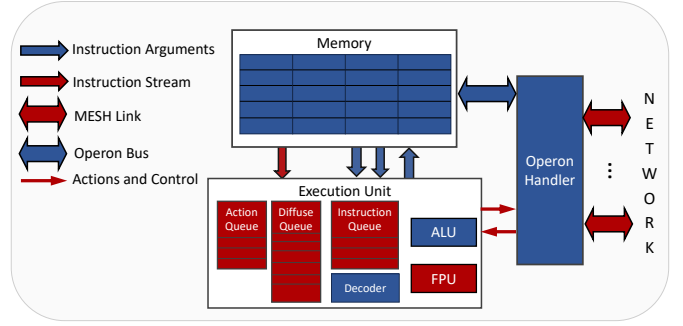
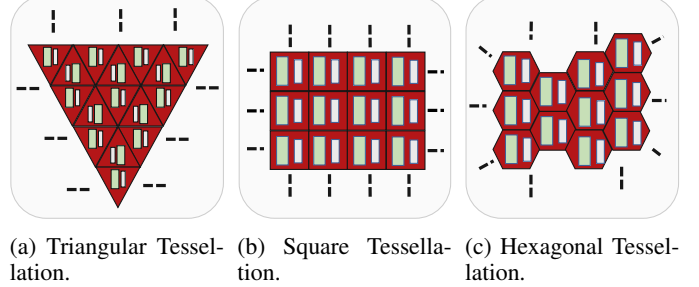


Fig. 3: Internal components of the AM-CCA compute cell.



(a) Triangular Tessellation. (b) Square Tessellation. (c) Hexagonal Tessellation.

Fig. 4: Tessellation of Compute Cells to form an AM-CCA chip.

#### A. Design Parameters for an AM-CCA Chip

The actual shape and capabilities of a single CC along with how these CCs are aggregated together to form a AM-CCA chip is a design compromise between three parameters: memory, compute, and communication. For a given area, in the theoretical limit, at the one end lies an infinite number of infinitesimally small CCs and at the other end there is only a single big CC encompassing the entire area. The latter can be synonymous to a conventional big core processor. In this sense there is a continuum from the very small to the large as depicted in Figure 5

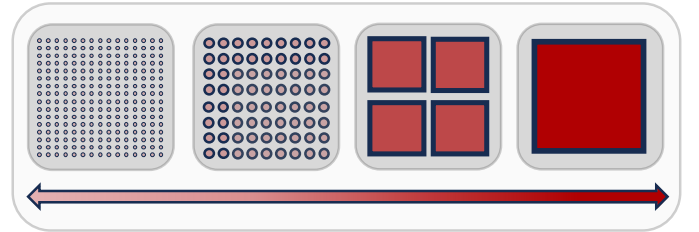


Fig. 5: Idea of the compute continuum. Storage and computation happens in a medium of active-memory computing cells. The medium can be a continuum of large number of tiny computing cells to a single big cell.

**1) Shape and Communication:** The shape of the CC determines its neighbor connectivity. For example, a CC that is shaped as an equilateral triangle can form three edges (connections) to its neighbors when placed in a 2D tessellation.



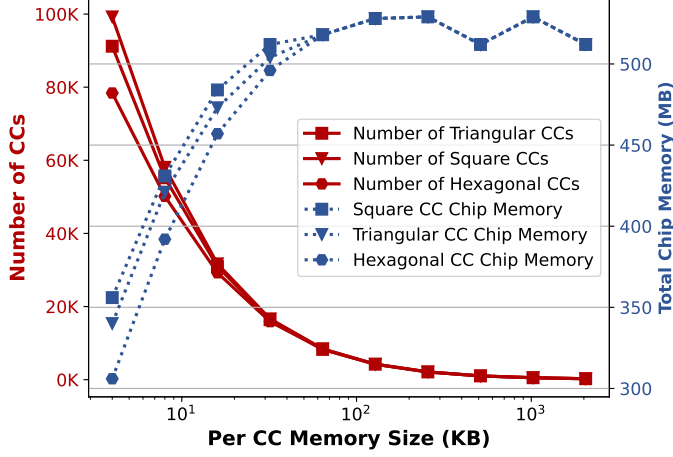


Fig. 6: Relationship between number of CCs and the total chip memory capacity, for various shapes, in under a  $300mm^2$  area AM-CCA chip. X-axis in log scale.

Other shapes can include: square with four edges, or hexagon with six edges. Shape of the CCs with more edges have higher communication bandwidth and operon parallelism at the cost of more die area. The cost of more edges per CC is a compromise against the size of memory per CC, compute logic per CC, and the overall number of CCs in the entire chip. Section III-A2 provides discussion on this trade-off space.

The shapes are not limited to regular tilings and 2D tessellations, as shown in Figure 4. There can be other complex non-regular tilings and 3D stacked tessellations; however, they are beyond the scope of this paper.

2) **Memory and Compute:** A single CC contains a limited amount of SRAM memory along with some computational ability. The capacity and capability of memory determines how much percent of die area is allocated to memory. There can be added capabilities of the memory, like mechanism for tag and its resolution to infer the type of an object at runtime. Likewise, a CC has a limited number of computational resources such as arithmetic unit and other functional units that occupy the die space. Increasing these resources will either come at the expense of less memory capacity and/or capability, and/or communication logic, and/or the total amount of CCs in a single AM-CCA chip.

To evaluate the impact of individual CC component sizes on the overall compute and communication capabilities of the AM-CCA chip in a practical scenario, we estimated transistor counts related to primary functional units of the cell. The derivation of relevant geometric parameters assumed a TSMC N5 (5nm) process for chip implementation with the effective transistor density of  $130 \text{ million/mm}^2$ , calculated using Apple M1 Ultra as a representative example. The central component of CC is a dual-port SRAM with 8T bitcells, structured as 4 independently addressed banks with 64-bit data I/O each and yielding a flit size of 256 bits for operon contents transfer



Fig. 7: All objects, whether user-defined or system objects, inherit from a base class containing the tag.

every clock cycle. While the memory I/O width remains constant in experiments, the address size is changed to reflect different memory capacities per CC along with corresponding transistor counts for address decoder, bit line drivers, sense amps, and output registers. The execution unit consists of instruction queue, instruction decoder, scalar ALU and FPU, and execution logic. All but the last require a fixed number of transistors of about  $100K$  in aggregate; execution logic changes are due to different address register widths determined by the cell's memory size. The execution unit connects to the SRAM block via 64-bit wide multiplexers that enable fetching instruction operands from any of the 4 memory banks and permit delivery of ALU/FPU result to any of the banks. Finally, mesh links, their associated FIFO storage, flit multiplexers, and router logic are analyzed. The transistor count here varies due to FIFO depth and number of outgoing links. While other combinatorial logic, such as various state machines, handshake and arbitration support, etc. was not included in the totals, its impact likely does not exceed 1–2%.

Using the above estimates, Figure 6 shows a relationship between the total number of compute cells and the resultant total memory of a AM-CCA chip inscribed in under  $300mm^2$  area. It shows the trade-off space between the amount of compute parallelism and the total chip memory capacity when per CC memory is increased.

#### IV. DATA STRUCTURE AND MEMORY MANAGEMENT

All memory allocations in AM-CCA are objects that derive from a common base class containing metadata of the object in a tagged region. Figure 7 shows the structure of an object. In the tag, each object contains its type information, pointer data such as count of references for potential garbage collection and object migration, access modes such as read and/or write, terminator detector related data that not only keeps track of the activation status of the object but also can allow for multiple user applications or system operations to act upon the object, and finally, some space for any user-defined metadata.

##### A. Graph Representation

A number of CCs may be needed to represent a single graph vertex, which can potentially have thousands or more edges along with other associated data, such as vertex ID, type, assigned values, and more. This is in part due to an individual CC having a limited amount of memory to hold large vertices. It is also to enable parallelism for a single vertex operation since the vertex is now divided and spans across multiple CCs. To achieve this we designed a datastructure called the Recursive Parallel Vertex Object (RPVO), shown in Figure 8 for the vertex in Figure 1a.

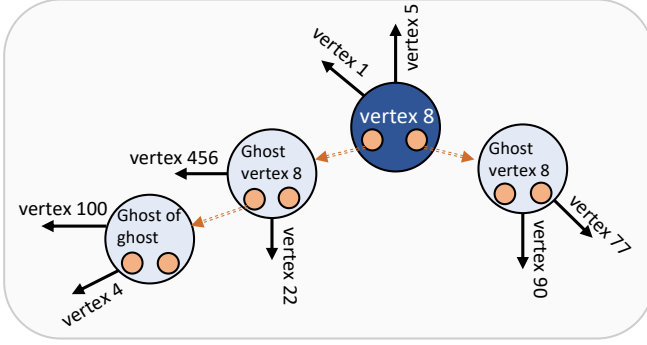


Fig. 8: Recursively Parallel Vertex Object.

The RPVO is constructed from vertex objects that are linked together hierarchy. These vertex objects contain a chunk of edges, called *local edge list*, stored as pointers to other RPVOs representing other vertices of the graph. The root vertex object serves as the user program’s accessible address for the vertex. In addition to containing a chunk of edges, the root vertex also holds program data defined by the user. On the other hand, the remaining vertex objects are referred to as *ghost vertices*, and they only contain chunks of edges and pointers to other ghost vertices within the hierarchy.

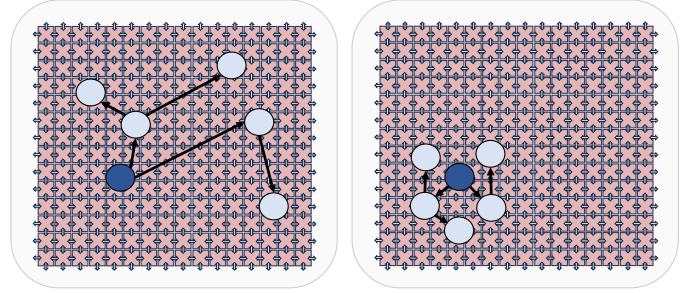
The child ghost vertices do not wait for parent ghost vertices. When a ghost vertex relays an *action* to its child ghost vertex on a different CC, the child can start execution as soon a resources are available at that CC. In this way, logically all vertices (root and ghost) of the RPVO can execute work in parallel.

The RPVO representation allows scaling the maximum size of a single vertex object beyond the memory limits of a single compute cell (or a tile, in the parlance of similar works). On top of that it also provides recursive parallelism for vertex operations. For example, edge search instead of being  $\mathcal{O}(\text{edges})$  now becomes  $\mathcal{O}(\log_g \text{depth} \times \text{local edge list size})$ , where  $g$  is the number of ghost vertices per vertex. Finally, the RPVO provides graceful mutations to the graph structure. Since vertices and edges are pointers they can be created, deleted, or modified on the fly. This is in contrast to more rigid matrix oriented representations such as the Compressed Sparse Row (CSR).

### B. Ghost Vertex Allocation Policy

We developed two ghost vertex allocation policies: *Random Allocator* and *Vicinity Allocator*, conceptually shown in Figure 9. As the name implies, the *Random Allocator* randomly allocates ghost vertices on any CC across the entire chip, whereas the *Vicinity Allocator* randomly allocates ghost vertices nearby<sup>1</sup>, aiming to reduce the latency of intra-vertex operations.

<sup>1</sup>In a real deployable system this memory allocation might be implemented using iterative deepening search originating from a CC to its radius set by the iterative deepening. Continuation will return the memory pointer to the calling CC.



(a) Random Allocator.

(b) Vicinity Allocator.

Fig. 9: Ghost vertex allocation policies: (a) allocate ghost vertices in compute cells nearby, (b) allocate ghost vertices randomly on the entire AM-CCA chip.

If two or more ghost vertices for a single vertex are allocated on the same CC, it may result in the serialization of recursive (hierarchical) parallelism. To minimize the probability of serialization when using the *Vicinity Allocator*, the radius of allocations, originating from the ghost vertex location, must be large enough to ensure that ghost vertices are allocated in distinct CCs as much as possible.

**Vicinity Radius vs Chip Size:** For smaller chip sizes and with large graphs containing high out-degree vertices the *Vicinity Allocator* will tend to be more like *Random Allocator*. This is because vertices with a large number of edges need to be partitioned across the smaller chip, and will end up being allocated across most of the chip. In is paper, we hardcode RPVO vertex to have the same vicinity radius for all vertices of a single input data graph. Future work can explore ways to self adjust the vicinity radius for each individual vertex, which may yield better performance. Section VI-C compares performance of *Vicinity Allocator* against *Random Allocator*.

Listing 1: SSSP Action

```
1 // Runtime knows the type of object 'this' from tag
2 SSSP_Action(int incoming_distance):
3     # Predicate
4     if this->distance > incoming_distance:
5         # Work
6         this->distance = incoming_distance;
7         # Diffuse
8         for (e in this->outbound_edges):
9             AMCCA_diffuse(e.vertex_addr,
10                           this->terminator,
11                           SSSP_Action(this->distance +
12                                         e.weight));
```

## V. DIFFUSIVE PROGRAMMING MODEL

Here we introduce what can be called the “*diffusive computing model*”, where an asynchronous action is sent from a memory locality to another memory locality (target). This action can mutate the state of the target locality and can further create new actions (work) at the destination thereby creating a ripple effect. Since the computation progresses asynchronously and has the potential to reactivate a previous node in the execution graph, this means that there is no predetermined computational dependency graph [22] or one

that is determined at runtime [26]. In asynchronous graph processing, there is no dependency graph or the Directed Acyclic Graph (DAG) of the execution. It is primarily because of arbitrary structure of the input data graph with arbitrary weights, whereby the execution (program) relies on some arbitrary invariant to advance [13]. Finally, such computations present an extra challenge of detecting when the execution is complete, known as the Termination Detection Problem (TDP). This problem does not manifest in formulations of the BSP counterparts.

Listing 2 shows a typical call to a AM-CCA diffusive program in a manner of an accelerator. It solves the Single Source Shortest Path (SSSP) using the SSSP\_Action of Listing 1.

Listing 2: Typical call to a diffusive computation

```

1 void main() {
2   Graph_Type Graph = /* Create the graph and
3                       allocate on the device */
4   int root = 42;
5   int distance = 0;
6   // Get address of the root vertex
7   AMCCA_Address root_addr = get_addr_at(Graph,
8                                         root);
9   // Create a terminator
10  AMCCA_Terminator sssp_terminator =
11    AMCCA_create_terminator();
12  // Create the action object
13  AMCCA_Action sssp_action =
14    AMCCA_Action(root_addr,
15                sssp_terminator,
16                SSSP_Action(distance));
17  // Germinate the action on the compute cell
18  // where root_addr exists
19  AMCCA_germinate_action(sssp_action);
20  // Diffuse and wait on terminator
21  AMCCA_run(sssp_terminator);
22 }

```

### A. Termination Detection

For the purposes of termination detection, Dijkstra–Scholten algorithm [7] is employed that creates an implicit spanning tree containing the set of active vertex objects. As the computation comes to an end, the spanning tree naturally unfolds and becomes empty, signifying termination. In a static spanning tree, such signal (or data) transmission from leaves to root is referred to as *convergecast* [25]. The difference here is that the spanning tree itself is dynamic and therefore it grows and shrinks as the computation progresses, acting as a hybrid between *convergecast* and *breadth-first traversal*. From an overhead perspective, the Dijkstra–Scholten’s termination detection requires sending an additional acknowledgment message for every application active message. This overhead on performance is studied in Section VI-B. Typically the programmer has to write the termination detection logic as part of the action code, thus increasing code complexity and denying the runtime system to separate these system tasks from application tasks. This logical separation may potentially allow the hardware and the runtime system to dedicate hardware termination detection units and methods for low overhead and increased performance. Therefore, we make the termination task first

class by providing an object called `AMCCA_Terminator` that serves as a link between the application code and the runtime system, managing termination of diffusion.

### B. Predicate and Work Pruning

Likewise, we make the predicate logic first class so that it becomes an innate part of the *action*, thus enabling the runtime system or hardware mechanism to schedule actions intelligently at the receiving locality. Think of multiple SSSP *actions* received for a single vertex object. Among these actions, only one may contain a better path to the solution based on some heuristic, in this case, the distance contained in its predicate. This particular action subsumes the work of all other actions, which are then discarded.

In the design discussed in this paper, we export the predicate to the runtime system. When an action is executed from the action queue, its predicate is evaluated first. If the predicate returns true, then the action’s work is performed. Finally diffusion occurs and new actions are created and sent along the edges of the vertex. The programming model assumes an action, with its work and diffusion, to be an atomic unit of execution. Under the hood, the compiler and runtime system work together to separate work from diffusion, which is then passed to the *diffusion queue* with a slightly modified predicate containing the same operands. For example BFS work predicate is `my_level > incoming_level`, then the modified predicate for diffuse becomes `my_level == incoming_level`. This later step opens up two new opportunities: firstly, it allows actions to be executed without being logically tied to their diffusion, thereby allowing the computation to not block on network operations. Secondly, it allows to filter out diffusions at a later time during the execution when newer actions arrive with better solutions thereby subsuming (pruning) the diffusions too.

## VI. EXPERIMENTS

We developed a simulator using C++ to design and deploy asynchronous message-driven computations and understand the runtime behavior of AM-CCA configurations. The simulator is high-level enough to be programmed using the diffusive programming model described in Section V and yet low-level enough to simulate individual operon movements between CCs. In a single simulation cycle, an operon can traverse one hop from one CC to a neighboring CC. We make this assumption since AM-CCA channel links are 256 bit wide and can easily send the small *operons* of our tested applications in a single flit cycle. Simultaneously, a single CC, can perform either of the two operations: 1) a computing task, which is the predicate resolution and work in the user application action, or 2) the creation and staging of a new *operon*. These assumption are also similar to the ones made by the authors of Dalorex, which we compare against in section VI-D. The simulator is available at [2].

<sup>2</sup>to be cited after acceptance so as to adhere to the double blind policy

In the scope of this paper, we have implemented only the square-tessellated AM-CCA, as shown in Figure 4b, as it strikes a balance among the three tessellations discussed in Subsection III-A1. The simulator employs turn-restricted routing that is deadlock free and always traverses the minimal path between source and destination [16]. In the case of the Torus-Mesh network, virtual channels are added to guarantee deadlock freedom [27]. Owing to its simplicity, the turn-restricted routing can be implemented without the need for complex circuitry and algorithms in the CCs. These choices serve as a straightforward starting point in our exploration of the AM-CCA’s design space.

**Applications:** Using the simulator, we implemented static and dynamic graph search applications: Static-SSSP, Static-BFS, and Dynamic-BFS. The application are fully asynchronous meaning there is no waiting on the frontier to be explored before moving to the next frontier. Furthermore, there is no meaning of the conventional frontier. The computation is decentralized and vertices asynchronously explore the search space. We verify the results for correctness against known results found using NetworkX [17]. For fairness and consistency with Dalorex, we invoke the search from the root vertex set to vertex 0 because that is what the authors of Dalorex used in their experiments. We find that using a random vertex as the root (such as vertex 0) is faster across datasets on various chip configurations than using the vertex with the highest out-degree, an other practice employed for fairness and consistency.

**Datasets:** We perform our experiments using a combination of synthetic graphs, which include RMAT (generated using PaRMAT [21] with  $a = 0.45$ ,  $b = 0.25$ , and  $c = 0.15$ ) and Erdős-Rényi (generated using NetworkX), as well as real-world graphs. Table II provides details of the graph datasets used in our static graph experiments, containing key insights such as average SSSP length, and degree distributions, which have implications on application, datastructure, and system behavior. To make the SSSP meaningful, random weights are assigned to the edges of both synthetic and real-world graphs. For the graphs LJ, WK, AM, and R22, the weights were assigned by the authors of Dalorex. For R18, E18, LN, and WG, we assigned random weights in the interval  $[1, 5]$ . For Dynamic-BFS we use datasets from MIT’s Streaming GraphChallenge [20] [1].

#### A. Effects of Congestion

We provisioned a large AM-CCA chip of  $128 \times 128$ , containing  $16K$  compute cells tessellated in a Torus-Mesh with a diameter of 127. The rationale is that such an extreme-scale configuration will enable very high degrees of fine-grain hardware parallelism, which will be subsequently exported by the data structure to the application. In this way, the extreme scales will aid us as a probe into identifying the limits of our design space.

We identify that very high ingress of diffusion messages, dictated by the input graph out-degree distribution, if unchecked quickly creates congestion on the network with

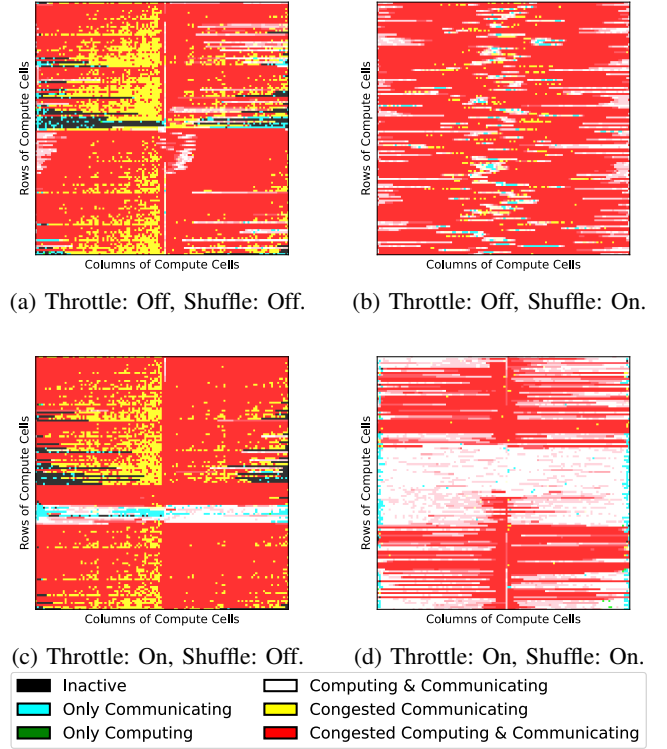


Fig. 10: A moment during the application run showing status per compute cell. There are  $128 \times 128$  compute cells with per virtual channel buffer size of 4 solving the Static-BFS of the RMAT-18 graph.

*operons* waiting on the network buffers, or action and diffusion queues. This ultimately leads to compute cells being unable to generate new *operons*, thereby stalling the computation. Although, as discussed in V-B, when a computation is stalled, we overlap it with filter passes on *action queue* and *diffuse queue* in the hope of work pruning; nevertheless, the network operations remain stalled.

Figure 10 visualizes a moment during execution of Static-BFS traversing the RMAT-18 graph. It shows the status of individual CCs, particularly highlighting whether they are congested. In Figure 10a and 10c, it is interesting to observe the emergence of the Kronecker recursive pattern from the congestion between CCs. However, as captivating as it may appear, its effects on performance are detrimental, as it keeps CCs either idle or congested more often. To remedy this, we shuffle the vertex list before allocation. Figure 10b and 10d show even-out traffic when vertices are shuffled. The horizontal pattern of congestion signifies the static X-Y dimension order routing. Shuffling is only needed where graphs have pattern associated with their vertex naming (IDs). For example Erdős-Rényi graphs have no patterns and therefore do not require shuffling. For consistency, we use shuffling in all our experiments.

To alleviate congestion and prevent *operons* from blocking



TABLE II: Details of the Static Input Data Graphs

Graph Name	Vertices	Directed Edges	SSSP Length ( $l$ )		In Degrees ( $k_{in}$ )				Out Degrees ( $k_{out}$ )			
			$\mu$	$\sigma$	$\mu$	$\sigma$	max	$\langle \%, \%tile \rangle$	$\mu$	$\sigma$	max	$\langle \%, \%tile \rangle$
language: LN	399.1 K	1.22 M	7.5	1.7	3.0	3.9	107	$\langle 99\%, 17 \rangle$	3.0	20.7	11.6 K	$\langle 99\%, 20 \rangle$
amazon0302: AM	262.1 K	1.23 M	8.8	1.8	4.7	5.7	420	$\langle 99\%, 23 \rangle$	4.7	0.9	5	$\langle 99\%, 5 \rangle$
Erdős-Rényi: E18	262.1 K	2.36 M	4.6	0.5	9.0	3.0	25	$\langle 99\%, 17 \rangle$	9	3.0	25	$\langle 99\%, 17 \rangle$
RMAT: R18	262.1 K	4.72 M	3.3	0.5	18.1	63.3	7.5 K	$\langle 96\%, 87 \rangle$	18.1	17.6	488	$\langle 96\%, 55 \rangle$
web-Google: WG	916.4 K	5.11 M	6.4	1.7	5.8	39.2	6.3 K	$\langle 96\%, 23 \rangle$	5.8	6.5	456	$\langle 96\%, 19 \rangle$
LiveJournal: LJ	4.85 M	68.99 M	-	-	14.2	43.4	13.9 K	$\langle 98\%, 99 \rangle$	14.2	36.0	20.3 K	$\langle 98\%, 98 \rangle$
Wikipedia: WK	4.21 M	101.31 M	-	-	24.0	412.9	431.8 K	$\langle 98\%, 152 \rangle$	24.0	47.8	8.1 K	$\langle 98\%, 129 \rangle$
RMAT: R22	4.19 M	128.31 M	-	-	30.5	345.6	162.8 K	$\langle 98\%, 308 \rangle$	30.5	345.6	162.8 K	$\langle 98\%, 308 \rangle$

$\mu$  is mean,  $\sigma$  is standard deviation, and the pair  $\langle \%, \%tile \rangle$  represents percentile % and its value %tile.

$l$  is found by averaging SSSP length of a sample of 100 vertices. K is thousand, and M is million.

R22 is undirected but represented as directed, hence exhibiting symmetry in out-degrees and in-degrees.

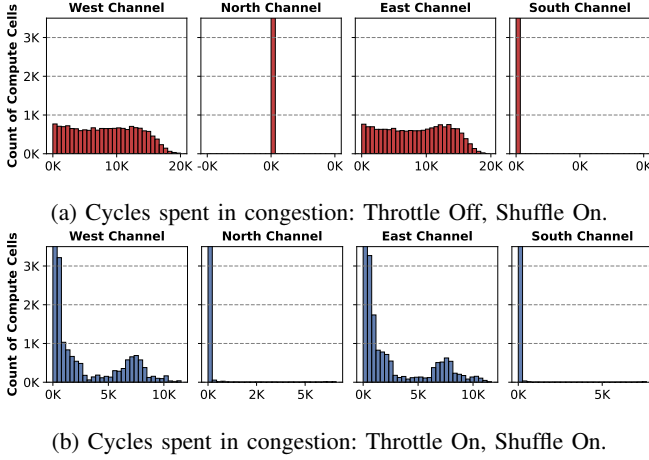


Fig. 11: Histogram of contention experienced per channel for all compute cells. There are  $128 \times 128$  compute cells with per virtual channel buffer size of 4 solving the Static-BFS of the RMAT-18 graph. Predictably, the west and east channels are highly contented due to the X-Y dimension order routing.

on the network, we implemented two strategies: throttling, and buffers. Under throttling the source of congestion is considered to be the presence of large amount of operons that overwhelm the network. Whereas, under buffering it is considered an issue of a single channel blocking on a single channel.

**Throttling:** We employ a simple mechanism. When a compute cell generates new operons, it first checks for congestion with its immediate neighbors for the previous cycle. Based on congestion, it halts the creation of any new operons for a set period of cycles  $T$ , in a hope to cool down the network. Equation 1 shows the hypotenuse of the chip, which is used as the throttling period  $T$ .

$$T = \begin{cases} \sqrt{dim_x^2 + dim_y^2} & \text{if Mesh} \\ \frac{\sqrt{dim_x^2 + dim_y^2}}{2} & \text{if Torus-Mesh} \end{cases} \quad (1)$$

When enabled, throttling relieves the constant operon pressure on the network. This can be visually seen in Figure 10d and yields a geometric mean improvement of  $1.5\times$  with

buffer size of 1 across datasets E18, R18, AM, LN, and WG. However, as depicted in Figure 10d, some congestion can still be seen, especially in horizontal chunks. This congestion is attributed to the nature of the Torus-Mesh network and the routing algorithm used, which relies on static horizontal first dimension order routing.

**Buffering:** We employed buffers at each virtual channel receive port of the compute cell. The buffers hold operons and allow the operon handler the freedom to route different operons when there is an open link. Figure 12 shows the impact of different buffer sizes, specifically 1, 4, and 8, on the time to solution.

*Effect of Buffers:* To isolate the individual effects of buffering and throttling, we varied the buffer sizes while keeping throttling turned off and turned on. In the first case, the buffers yielded a performance improvement of geometric mean  $1.15\times$  and  $1.28\times$  for buffer sizes 4 and 8, respectively. In the second case, when throttling was turned on and buffer sizes were increased, we observed a similar geometric mean improvement of  $1.18\times$  and  $1.26\times$  for buffer sizes 4 and 8, respectively. Figure 11 shows histogram of contention experienced per channel for all compute cells. Due to the horizontal (X-Y) dimension order routing, the west and east channels experience high contention, as depicted in Figure 11a. Although throttling reduces contention on these channels, as shown in Figure 11b, there is still room for adaptive routing and less aggressive throttling algorithms that can better utilize available buffers for performance improvements.

When combined together buffers and throttling yield a geometric mean performance improvement of 1.5, 1.78, and 1.92 for buffer sizes of 1, 4, and 8, respectively. Figure 12 provides detailed data.

**Blocking Techniques:** There are blocking methods available to mitigate the issue of congestion, such as message coalescing and message reduction in the Active Pebbles system [35]. Message coalescing involves grouping the messages before sending at the expense of making the application a little coarser, and message reduction involves staging and processing messages at the sender in a hope to reduce redundant messages aimed at a single receiver. However, we did not choose to implement these blocking methods as the purpose

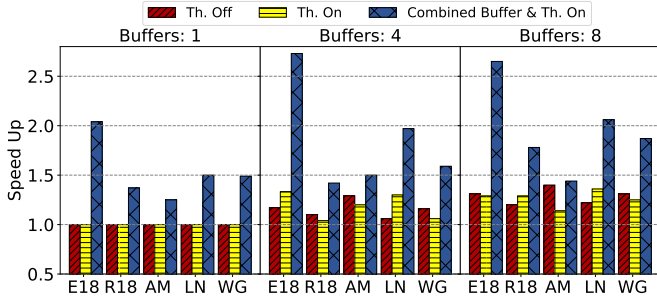


Fig. 12: Effect of throttle and buffers on performance. **Throttle Off** and **Throttle On** compares only the effect of buffers with respect to their buffer size of 1. **Combined Throttle and Buffer** compares the performance improvement with throttle On and buffers with respect to throttle Off and buffer size of 1.

of our experiments is to expose, exploit, and understand unbounded parallelism. Using blocking techniques would limit the amount of instantaneous parallelism and defeat the purpose of this endeavor.

#### B. Overheads of Termination Detection

The Dijkstra–Scholten termination detection used generates double the amount of actions, one per application action in the form an operon containing the acknowledgement message, thus creating double the work. This is coupled with the symmetric routing path that the acknowledgement operon must take under dimension order routing, contributing to congestion in the same region. To isolate the effects of termination detection on the performance we ran AM-CCA with Dijkstra–Scholten termination detection and again with simulating a conventional hierarchical signaling mechanism. In the latter scenario, the host receives an interrupt signal when all action queues, diffusion queues, operon buffers, and links are empty, indicating termination. In this mode, AM-CCA behaves like an accelerator surrendering its capabilities of a system on its own. In the scope of this paper, this is justifiable in that we are not invoking any runtime system tasks such as introspection, object migration, garbage collection, or multiple user applications, to name a few.

Termination detection had a performance overhead of around  $2\times$  across datasets, correlating with twice the operons generated due to the Dijkstra–Scholten algorithm. Since the termination detection is not part of the computation proper, the messages it generates can be predicted, reduced, and implemented by dedicated hardware units with potentially special network links. The blocking and reduction techniques of Active Pebbles can come to rescue without sacrificing on the fine-grain parallelism because these messages are not part of the application parallelism.

#### C. Effects of Object Allocation Policy

By aligning the recursive parallelism of RPVO to the spatial locality of compute cells the vicinity allocator achieves a

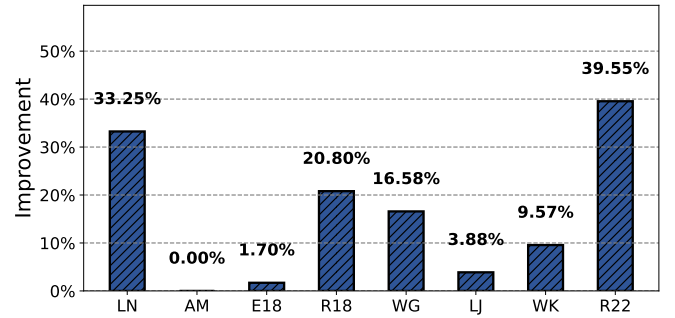


Fig. 13: Performance of Vicinity Allocator vs Random Allocator: Static-BFS on  $128 \times 128$  compute cells.

significant performance improvement for graphs that have vertices with thick and/or skewed outdegree distribution. In our experiments these were the R18, R22, and WK graphs with thick mean of outdegree edges. Figure 13 shows performance improvement across datasets. The AM graph had a 0% improvement owing to no recursive parallelism with the *local edge list size* being too small to warrant any ghost vertices. Excluding AM, the vicinity allocator yields a geomean speed up of  $1.23\times$  across datasets.

**Limitations:** The RPVO format provides a single target for in-degree edges thus causing high ingress load at a single compute cell or vertex. New techniques must be explored that, like sharing the out-degree load as ghost vertices does, also share the in-degree load.

#### D. Comparison against state-of-the-art

We compare AM-CCA against Dalorex [29], an state-of-the-art similar work. It is a cache-less architecture, where new tasks spawn at each memory indirection. These tasks are then sent for execution to the cores where the data resides. Like AM-CCA, its programming model and execution can support fully asynchronous computations without any global barriers. Unlike AM-CCA with object pointer and actions, it uses CSR format with loop based programming constructs that make it less flexible for dynamic graph computations.

We acquired the Dalorex’s experiment logs from the authors along with the exact datasets that they used. Dalorex simulator [30] operates under similar assumptions, compared to our simulator, regarding work and communication. AM-CCA was set in accelerator mode by disabling the Dijkstra–Scholten termination detection mechanism.

Figure 14 shows AM-CCA’s graph traversal (Static-BFS) and search (Static-SSSP) performance compared to Dalorex across datasets for three chip sizes:  $16 \times 16$ ,  $32 \times 32$ , and  $64 \times 64$ . AM-CCA achieves a geomean speed up of  $2.38\times$  for Static-BFS and  $2.11\times$  for Static-SSSP across datasets and chip sizes. At large chip sizes, beyond  $32 \times 32$ , Dalorex augments Torus-Mesh with Ruche links for lower diameter and latency. AM-CCA does not use any Ruche links and solely relies on Torus-Mesh to scale. For chip size of  $64 \times 64$ , AM-CCA is geomean  $2.33\times$ , and  $2.03\times$  faster for (Static-BFS) and search (Static-SSSP), respectively.

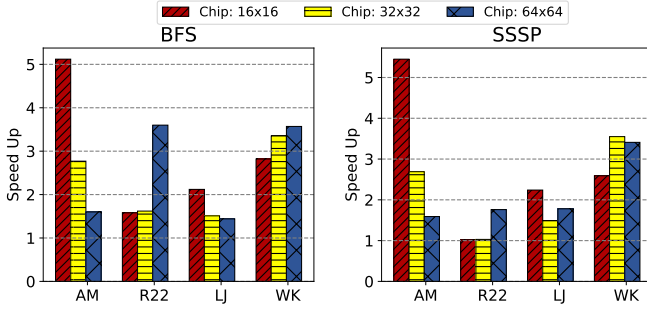


Fig. 14: Speed up vs. Dalorex: Compares number of simulation cycles.

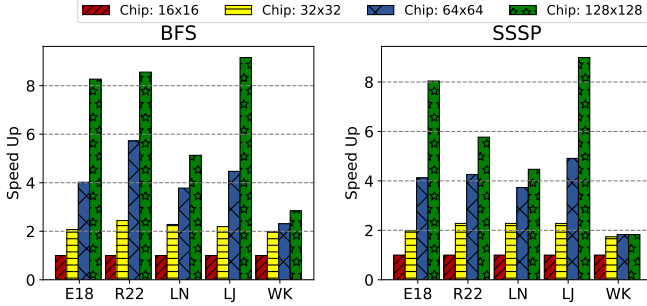


Fig. 15: Strong scaling of AM-CCA.

Furthermore, Figure 15 shows AM-CCA scaling beyond  $64 \times 64$  to  $128 \times 128$  with 16K compute cells. The graph with heavy in-degree distribution relative to out-degree, such as WK, did not scale better at larger chip sizes. As mentions earlier, new techniques much be explored that evolve RPVO to also be able to parallelized in-degree edge loads. One future direction can to be depart from pure tree like structures, which the RPVO is, and incorporate structure and features of Rhizomes.

#### E. Dynamic Graphs

AM-CCA is natively designed to support dynamic graph processing using programming abstractions of *actions*, dynamic storage scheme of RPVO, and message delivery of *operons* that contain continuations. An *operon* carrying edge(s) for insertion can be coupled with a continuation that spawns new *action* thus enabling dynamic graph processing. We implement Dynamic-BFS using contiutions. When a new edge is inserted the continuation spawns an *action* that sends BFS level along the newly added edge. In this way, Dynamic-BFS reuses prior results from prior computation without needing to compute levels for each and every vertex from scratch.

Figure 16 compares performance of Dynamic-BFS against Static-BFS using input data from GraphChallenge that has 200K vertices with initially 475K edges. At each increment about 475K new edges are added to the graph. Static-BFS computes BFS at each increment from scratch while Dynamic-BFS reuses prior state. Dynamic-BFS provides a geomean speedup of  $2.29\times$  for all nine increments. If we split the increments into two, Dynamic-BFS achives a geomean speed

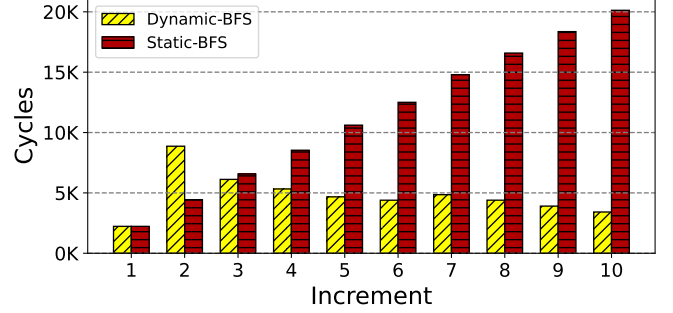


Fig. 16: Comparison of Dynamic-BFS and Static-BFS performance on a  $64 \times 64$  AM-CCA chip. Each increment represents an insertion of 475K new edges to a graph with 200K vertices.

up of  $1.18\times$  for the first four increments but later as the graph evolves and becomes larger, we observe a geomean speed up of  $3.90\times$  for the last five increments.

## VII. CONCLUSION

AM-CCA aims to provide a unified approach to system design for irregular memory applications such as graph processing. It achieves this by providing architectural support for massive fine-grain message-driven computations that send actions carrying the work to data. This underlying raw parallelism is transparently exported to the application by the means of an asynchronous programming model and a runtime system that manage an inherently parallel and dynamic object model as the data structure of the irregular input graph. Simulated experimental results show performance gain of geomean  $2.38\times$  against an state-of-the-art similar system for graph traversals and yet being able to natively support dynamic graph processing. It uses programming abstractions of actions, introduces new dynamic graph storage scheme, and message delivery mechanisms with continuations that contain post-completion actions. Continuations seamlessly adjusts prior or running execution to mutations in the input graph and enable dynamic graph processing.

AM-CCA also paves the way for future work in areas of 1) dynamic object migration on the fine-grain medium composed of compute cells, 2) low overhead techniques for system tasks such as termination detection, 3) data allocation policies and algorithms for the Recursively Parallel Vertex Object (RPVO) that are synchronization free, and 4) better congestion management.

## ACKNOWLEDGEMENTS

**To be added:**

## REFERENCES

- [1] "Data Sets — GraphChallenge — graphchallenge.mit.edu," <https://graphchallenge.mit.edu/data-sets#PartitionDatasets>, [Accessed 14-01-2024].
- [2] G. Agha, *Actors: A Model of Concurrent Computation in Distributed Systems*. Cambridge, MA, USA: MIT Press, 1986.

- [3] J. Ahn, S. Hong, S. Yoo, O. Mutlu, and K. Choi, "A scalable processing-in-memory accelerator for parallel graph processing," in *2015 ACM/IEEE 42nd Annual International Symposium on Computer Architecture (ISCA)*, 2015, pp. 105–117.
- [4] Arvind and D. E. Culler, "Dataflow architectures," *Annual Review of Computer Science*, vol. 1, no. 1, pp. 225–253, 1986. [Online]. Available: <https://doi.org/10.1146/annurev.cs.01.060186.001301>
- [5] J. Backus, "Can programming be liberated from the von neumann style? a functional style and its algebra of programs," *Commun. ACM*, vol. 21, no. 8, p. 613–641, aug 1978. [Online]. Available: <https://doi.org/10.1145/359576.359579>
- [6] M. Brodowicz, T. Sterling, and M. Anderson, "Continuum computing - on a new performance trajectory beyond exascale," *Supercomputing Frontiers and Innovations*, vol. 5, no. 3, p. 5–24, Sep. 2018. [Online]. Available: <https://superfri.org/index.php/superfri/article/view/188>
- [7] E. W. Dijkstra and C. Scholten, "Termination detection for diffusing computations," *Information Processing Letters*, vol. 11, no. 1, pp. 1–4, 1980. [Online]. Available: <https://www.sciencedirect.com/science/article/pii/0020019080900216>
- [8] D. R. Ditzel and D. A. Patterson, "Retrospective on high-level language computer architecture," in *Proceedings of the 7th Annual Symposium on Computer Architecture*, ser. ISCA '80. New York, NY, USA: Association for Computing Machinery, 1980, p. 97–104. [Online]. Available: <https://doi.org/10.1145/800053.801914>
- [9] R. Duncan, "A survey of parallel computer architectures," *Computer*, vol. 23, no. 2, pp. 5–16, 1990.
- [10] S. E. Fahlman, "Marker-passing inference in the scone knowledge-base system," in *Proceedings of the First International Conference on Knowledge Science, Engineering and Management*, ser. KSEM'06. Berlin, Heidelberg: Springer-Verlag, 2006, p. 114–126. [Online]. Available: [https://doi.org/10.1007/1181220\\_11](https://doi.org/10.1007/1181220_11)
- [11] S. E. Fahlman, G. E. Hinton, and T. J. Sejnowski, "Massively parallel architectures for ai: Netl, thistle, and boltzmann machines," in *Proceedings of the Third AAAI Conference on Artificial Intelligence*, ser. AAAI'83. AAAI Press, 1983, p. 109–113.
- [12] E. A. Feustel, "On the advantages of tagged architecture," *IEEE Trans. Comput.*, vol. 22, no. 7, p. 644–656, jul 1973. [Online]. Available: <https://doi.org/10.1109/TC.1973.5009130>
- [13] J. S. Firoz, M. Zalewski, T. Kanewala, and A. Lumsdaine, "Synchronization-avoiding graph algorithms," in *2018 IEEE 25th International Conference on High Performance Computing (HiPC)*, 2018, pp. 52–61.
- [14] M. Flynn, "Very high-speed computing systems," *Proceedings of the IEEE*, vol. 54, no. 12, pp. 1901–1909, 1966.
- [15] R. P. Gabriel, *Performance and Evaluation of LISP Systems*. USA: Massachusetts Institute of Technology, 1985.
- [16] C. J. Glass and L. M. Ni, "The turn model for adaptive routing," in *Proceedings of the 19th Annual International Symposium on Computer Architecture*, ser. ISCA '92. New York, NY, USA: Association for Computing Machinery, 1992, p. 278–287. [Online]. Available: <https://doi.org/10.1145/139669.140384>
- [17] A. A. Hagberg, D. A. Schult, and P. J. Swart, "Exploring network structure, dynamics, and function using networkx," in *Proceedings of the 7th Python in Science Conference*, G. Varoquaux, T. Vaught, and J. Millman, Eds., Pasadena, CA USA, 2008, pp. 11 – 15. [Online]. Available: [http://conference.scipy.org/proceedings/SciPy2008/paper\\_2/](http://conference.scipy.org/proceedings/SciPy2008/paper_2/)
- [18] C. Hewitt, "Actor model of computation: Scalable robust information systems," 2010. [Online]. Available: <https://arxiv.org/abs/1008.1459>
- [19] D. C. Jung, S. Davidson, C. Zhao, D. Richmond, and M. B. Taylor, "Ruche networks: Wire-maximal, no-fuss nocs : Special session paper," in *2020 14th IEEE/ACM International Symposium on Networks-on-Chip (NOCS)*, 2020, pp. 1–8.
- [20] E. K. Kao, V. Gadepally, M. B. Hurley, M. Jones, J. Kepner, S. Mohindra, P. Monticciolo, A. Reuther, S. Samsi, W. Song, D. Staheli, and S. T. Smith, "Streaming graph challenge: Stochastic block partition," *CoRR*, vol. abs/1708.07883, 2017. [Online]. Available: <http://arxiv.org/abs/1708.07883>
- [21] F. Khorasani, R. Gupta, and L. N. Bhuyan, "Scalable simd-efficient graph processing on gpus," in *Proceedings of the 24th International Conference on Parallel Architectures and Compilation Techniques*, ser. PACT '15, 2015, pp. 39–50.
- [22] D. J. Kuck, R. H. Kuhn, D. A. Padua, B. Leasure, and M. Wolfe, "Dependence graphs and compiler optimizations," in *Proceedings of the 8th ACM SIGPLAN-SIGACT Symposium on Principles of Programming Languages*, ser. POPL '81. New York, NY, USA: Association for Computing Machinery, 1981, p. 207–218. [Online]. Available: <https://doi.org/10.1145/567532.567555>
- [23] K. Lakhota, M. Besta, L. Monroe, K. Isham, P. Iff, T. Hoefler, and F. Petrini, "Polarfly: A cost-effective and flexible low-diameter topology," in *Proceedings of the International Conference on High Performance Computing, Networking, Storage and Analysis*, ser. SC '22. IEEE Press, 2022.
- [24] N. Linial, "Distributive graph algorithms global solutions from local data," in *28th Annual Symposium on Foundations of Computer Science (sfcs 1987)*, 1987, pp. 331–335.
- [25] N. A. Lynch, *Distributed Algorithms*. San Francisco, CA, USA: Morgan Kaufmann Publishers Inc., 1996.
- [26] Q. Meng, A. Humphrey, J. Schmidt, and M. Berzins, "Investigating applications portability with the uintah dag-based runtime system on petascale supercomputers," in *Proceedings of the International Conference on High Performance Computing, Networking, Storage and Analysis*, ser. SC '13. New York, NY, USA: Association for Computing Machinery, 2013. [Online]. Available: <https://doi.org/10.1145/2503210.2503250>
- [27] Y. Miura, K. Shimozono, S. Watanabe, and K. Matoyama, "An adaptive routing of the 2-d torus network based on turn model," in *2013 First International Symposium on Computing and Networking*, 2013, pp. 587–591.
- [28] M. D. Noakes, D. A. Wallach, and W. J. Dally, "The j-machine multicomputer: An architectural evaluation," in *Proceedings of the 20th Annual International Symposium on Computer Architecture*, ser. ISCA '93. New York, NY, USA: Association for Computing Machinery, 1993, p. 224–235. [Online]. Available: <https://doi.org/10.1145/165123.165158>
- [29] M. Orenes-Vera, E. Tureci, D. Wentzlaff, and M. Martonosi, "Dalorex: A data-local program execution and architecture for memory-bound applications," in *2023 IEEE International Symposium on High-Performance Computer Architecture (HPCA)*. Los Alamitos, CA, USA: IEEE Computer Society, mar 2023, pp. 718–730. [Online]. Available: <https://doi.ieeecomputersociety.org/10.1109/HPCA56546.2023.10071089>
- [30] M. Orenes-Vera, E. Tureci, M. Martonosi, and D. Wentzlaff, "Muchisim: A simulation framework for design exploration of multi-chip manycore systems," 2023.
- [31] F. J. Pollack, G. W. Cox, D. W. Hammerstrom, K. C. Kahn, K. K. Lai, and J. R. Rattner, "Supporting ada memory management in the iapx-432," *SIGPLAN Not.*, vol. 17, no. 4, p. 117–131, mar 1982. [Online]. Available: <https://doi.org/10.1145/960120.801835>
- [32] T. Sterling and L. Bergman, "A design analysis of a hybrid technology multithreaded architecture for petaflops scale computation3," in *Proceedings of the 13th International Conference on Supercomputing*, ser. ICS '99. New York, NY, USA: Association for Computing Machinery, 1999, p. 286–293. [Online]. Available: <https://doi.org/10.1145/305138.305205>
- [33] T. von Eicken, D. E. Culler, S. C. Goldstein, and K. E. Schauer, "Active messages: A mechanism for integrated communication and computation," in *Proceedings of the 19th Annual International Symposium on Computer Architecture*, ser. ISCA '92. New York, NY, USA: Association for Computing Machinery, 1992, p. 256–266. [Online]. Available: <https://doi.org/10.1145/139669.140382>
- [34] D. Vortex, "Hpcc random access benchmark excels on data vortex™," White Paper, June 2016. [Online]. Available: <https://www.datavortex.com/wp-content/uploads/2017/05/HPCC-Random-Access-Benchmark-Excels-on-Data-Vortex.pdf>
- [35] J. J. Willcock, T. Hoefler, N. G. Edmonds, and A. Lumsdaine, "Active pebbles: Parallel programming for data-driven applications," in *Proceedings of the International Conference on Supercomputing*, ser. ICS '11. New York, NY, USA: Association for Computing Machinery, 2011, p. 235–244. [Online]. Available: <https://doi.org/10.1145/1995896.1995934>
- [36] S. Wolfram, "Cellular automata as simple self-organizing systems," 1982.